



Melt and collapse of buried water ice: An alternative hypothesis for the formation of chaotic terrains on Mars

Tanja E. Zegers^{a,*}, Jelmer H.P. Oosthoek^b, Angelo P. Rossi^c, Jan Kees Blom^d, Sandra Schumacher^e

^a Faculty of Geoscience, Department of Earth Sciences, Utrecht University, Budapestlaan 4, 3508 TA Utrecht, The Netherlands

^b TNO/Deltares, Geological Survey of the Netherlands, P.O. Box 80015, 3508 TA Utrecht, The Netherlands

^c International Space Science Institute, Hallerstrasse 6, CH-3012 Bern, Switzerland

^d Dept. of Applied Earth Sciences, Delft University of Technology, Stevinweg 1, 2628 CN Delft, The Netherlands

^e Solar System Missions Division, Research and Scientific Support Department of ESA, ESTEC, 2200 AG Noordwijk, The Netherlands

ARTICLE INFO

Article history:

Received 30 March 2010

Received in revised form 28 June 2010

Accepted 29 June 2010

Available online 31 July 2010

Editor: T. Spohn

Keywords:

Mars
chaotic terrain
heat flux
outflow channel

ABSTRACT

Chaotic terrains and the associated massive outflow channels are some of the most enigmatic features on Mars. Over hundreds of kilometres of rock units are fractured, tilted, and have subsided, forming chaotic terrain basins (Sharp, 1973). Large quantities of water emanated from these chaotic terrains in short periods of time in the Hesperian epoch (~3.7–3.3 Ga), carving huge outflow channels, thousands of kilometres long, and more than 1 km deep (Baker, 2001). However, the subsurface mechanism by which chaotic terrains form, and thereby suddenly produce very large quantities of water ($>10^5 \text{ km}^3$) is poorly understood. Here we explore if these features can form by melting and collapse of buried water ice in a confined basin. 2D thermal modelling, using boundary conditions derived from the geology of Aram Chaos, demonstrates that a buried ice unit will start melting when 1–2 km of overburden has accumulated. The thickness of the liquid subsurface layer depends primarily on the crustal heat flux, the thermal conductivity of the overburden sediments, and the surface temperature. A subsurface liquid water layer of 1 to 2 km can be achieved under present day surface temperature conditions and a crustal heat flux of 15–30 mW m^{-2} . To a first order, the geological features of chaotic terrains and their outflow channels are consistent with a scenario in which a subsurface lake forms by melting of buried water ice, followed by collapse and rapid outflow of water. If correct, this hypothesis suggests that subsurface lakes on Mars may have existed for extensive ($>100 \text{ Ma}$) periods of time. Such subsurface lakes would be of major interest for astrobiology.

© 2010 Elsevier B.V. All rights reserved.

1. Introduction

Martian chaotic terrains have a peculiar morphology with no obvious terrestrial equivalent. The common characteristics (Sharp, 1973; Chapman and Tanaka, 2002; Glotch and Christensen, 2005; Rodriguez et al., 2005b; Meresse et al., 2008) are irregular arrays of fractured and tilted blocks up to tens of kilometres in size, currently forming depressions in the landscape hundreds of meters deep. Chaotic terrains predominantly occur in the Martian highlands, south of Chryse Planitia, and generally border the dichotomy boundary with the northern lowlands. The location of chaotic terrains at the source of the Hesperian (~3.7–3.3 Ga) (Nelson and Greeley, 1999; Tanaka et al., 2003) catastrophic outflow channels (Carr, 1979, 1996; Baker, 2001) have led to a common general scenario: water is discharged from the subsurface and results in catastrophic outflow. However, the mechanism by which chaotic terrains form, and discharge catastrophic volumes of water has remained unclear.

Various chaotic terrains have been studied in detail using a combination of recent remote sensing data (Catling and Moore, 2003; Glotch and Christensen, 2005; Rodriguez et al., 2005b; Glotch and Rogers, 2007; Masse et al., 2008; Meresse et al., 2008; Noe Dobrea et al., 2008; Lichtenberg et al., 2010). Although all chaotic terrains have specific geological setting and characteristics, there is a commonality in the geological sequence of events associated with the formation of chaotic terrains (Sharp, 1973; Carr, 1980). The events which appear to be shared by all chaotic terrains are fracturing and tilting of the upper crustal units, associated with subsidence. With the topographic data from MOLA and HRSC Digital Elevation Models (DEM) the depression resulting from subsidence in chaotic terrains has been shown to be variable, but frequently up to 2 km (Meresse et al., 2008). The subsidence is commonly thought to be the result of expulsion of water from the subsurface. Some, but not all chaotic terrains show well developed catastrophic outflow channels which attest to the outflow of water from the chaotic terrain. An example of a chaotic terrain illustrating those features is Hydapsis Chaos (Fig. 1).

Some chaotic terrains are associated with light toned layered deposits. The light toned deposits do not show the fractures typical of chaotic terrains, and their deposition has been shown to post-date the

* Corresponding author. Tel.: +31 630395627; fax: +31 30243 1677.
E-mail address: tanja@geo.uu.nl (T.E. Zegers).

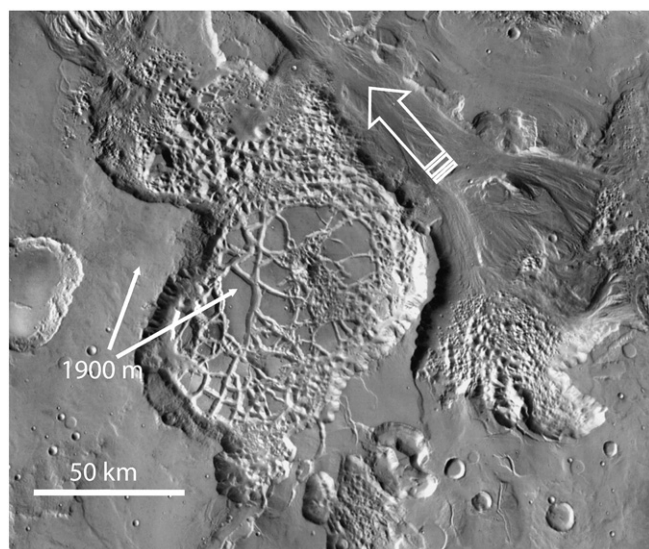


Fig. 1. View of Hydaspis Chaos (THEMIS IR day image, credit GoogleMars) showing the typical fractured and tilted chaos blocks, and associated outflow channels (thick arrow). The difference in elevation between the fractured chaotic terrain and the surrounding highlands is ~1900 m in this particular case.

formation of the chaotic terrain (Glotch and Christensen, 2005; Masse et al., 2008). An example is shown in Fig. 2 for Aram Chaos. Hematite is associated with such light toned layered deposits (Christensen et al., 2001), and recent hyperspectral data from OMEGA and CRISM instruments has indicated the occurrence of hydrated minerals, such as sulphate, goethite and other hydrated/hydroxylated Fe-oxides (Gendrin et al., 2005; Masse et al., 2008) in those deposits.

Various models have been proposed for the formation of chaotic terrains. In a first group of models, water is thought to be derived from partial melting and rupture of the cryosphere (Sharp, 1973; Chapman and Tanaka, 2002; Rodriguez et al., 2005b; Meresse et al., 2008), the upper 3 to 5 km of the crust, where pore space is entirely filled with ice. To initiate melting of the cryosphere, subsurface magmatic intrusions are generally invoked. Whereas most workers assume that water ice is present in fine-scale (mm–cm) porespace or fractures (Clifford, 1993), Rodriguez et al. (2005a) suggested that the subsurface of Mars contains an accumulation of impact craters and associated fracture systems, and some of those large or interconnected craters may have been partly filled with water, either liquid or ice. Such “cavernous” systems may then result in large scale subsidence if liquid water is released to the surface. In an extreme case, one could envisage that a water ice unit, unsupported by a rocky matrix or surrounding cave walls, is present in the subsurface. An analogue sand-box experiment (Manker and Johnson, 1982) illustrates that morphologies similar to chaotic terrains form by local melting of such a confined subsurface water ice unit. In the simulations, collapse features did not result from local melting of a stratigraphy containing ground ice (soil with ice in the pore space).

In a second group of scenarios, water is thought to be situated in a global pressurized sub-cryospheric aquifer (Clifford, 1993), and is released to the surface (Carr, 1979) by cryosphere rupture. Numerical flow models (Andrews-Hanna and Phillips, 2007; Harrison and Grimm, 2008) indicate that the large total liquid water volumes (10^5 – 10^6 km³) and high discharge rates (10^6 – 10^9 m³ s⁻¹) required to form the morphology of the outflow channels emerging from chaotic terrains (Baker, 2001) are not achievable by a single discharge from a porous medium. To still achieve the erosive power required to form the outflow channels from melted cryosphere or aquifers, a scenario was proposed (Harrison and Grimm, 2008) where a large number of flooding events (>100) and temporary ponding is followed by sudden release of water.

As an alternative to the release of water stored in the crust as liquid water or ice, it has been proposed that chaotic terrains and outflow features may be the result of the release of water stored in the mineral lattice of either evaporates (Montgomery and Gillespie, 2005) or in gas-hydrates (Max and Clifford, 2001). Those models require large volumes of evaporates or gas-hydrates in the subsurface, since the fraction of water in the mineral lattice is small (16 to 50%). To cause the dehydration reaction, heating is required.

Here we explore the hypothesis in which a chaotic terrain may form by melting of a buried unit of water ice. We consider this hypothesis for the Aram Chaos terrain, and study, using a numerical model, the thermal behaviour of a buried ice unit under relevant Martian surface and subsurface conditions. We show that melting of a buried unit of ice can occur, even in the absence of an external thermal event (e.g. volcanism, intrusion), as a combined consequence of the ambient crustal heat flux and the thermal insulation by the overburden sediments.

2. Conceptual model

The three first order observations of chaotic terrains are 1) fractured crustal block ranging in size between tens of kilometres to fracture blocks below the imaging resolution (several meters), 2) the fractured chaotic terrains form depressions, generally thought to be the result of subsidence during the fracturing event (Carr, 1980; Glotch and Christensen, 2005; Rodriguez et al., 2005a; Meresse et al., 2008), and 3) indications for outflow of water through outflow channels. All these features are present in Aram Chaos (Fig. 2). Whereas for most chaotic terrains the subsurface geometry can only be speculated on, for Aram Chaos it is likely that the circular shape of the chaotic terrain resulted from an original large impact crater geometry (Glotch and Christensen, 2005). This makes it possible to develop a conceptual model for the evolution of the Aram Chaos terrain, assuming the extreme case where the chaotic terrain formed by collapse as a result of melting of a subsurface ice unit, following the suggestion by (Manker and Johnson, 1982).

Fig. 3 illustrates the conceptual scenario for Aram Chaos. The initial condition is a large (280 km diameter) impact crater in the highland terrain of Mars. This crater is partly filled with water ice, and subsequently filled in with sediments and possibly volcanic ash. If the ice in the subsurface melts, it will eventually reach a point of instability and the rocky overburden collapses. If the water flows out, a channel will be carved. If the water evaporates, a chaotic terrain without an outflow channel will remain. If the water freezes in the basin, at the surface only a flat filled crater will be visible. For Aram Chaos, with a well developed single outflow channel, the first option seems most applicable.

3. Boundary conditions

We used the Aram Chaos terrain to reconstruct some of the boundary conditions which were subsequently used in the numerical modelling of the thermal state of a buried ice unit. A topographic cross-section of the current situation, based on MOLA data, is shown in Fig. 4. We modelled the original depth of a crater with the size of the Aram Chaos crater using an empirical relation between crater diameter and depth (Parker et al., 2010). Craters can be modelled with the curve H (m) = $350 D^{0.44}$, which gives us the best available estimate for the apparent depth of “pristine” craters. For Aram Chaos, with an estimated diameter of 280 km, this results in an original depth of 4177 m. In Fig. 4 the modelled outline of the original impact crater in the subsurface is shown with a dashed line.

Following the scenario illustrated in Fig. 3, the amount of subsidence of the fractured terrain equals the thickness of the liquid water layer prior to collapse. In the case of Aram Chaos, we do not know if the crater was entirely filled prior to collapse. If, as an extreme

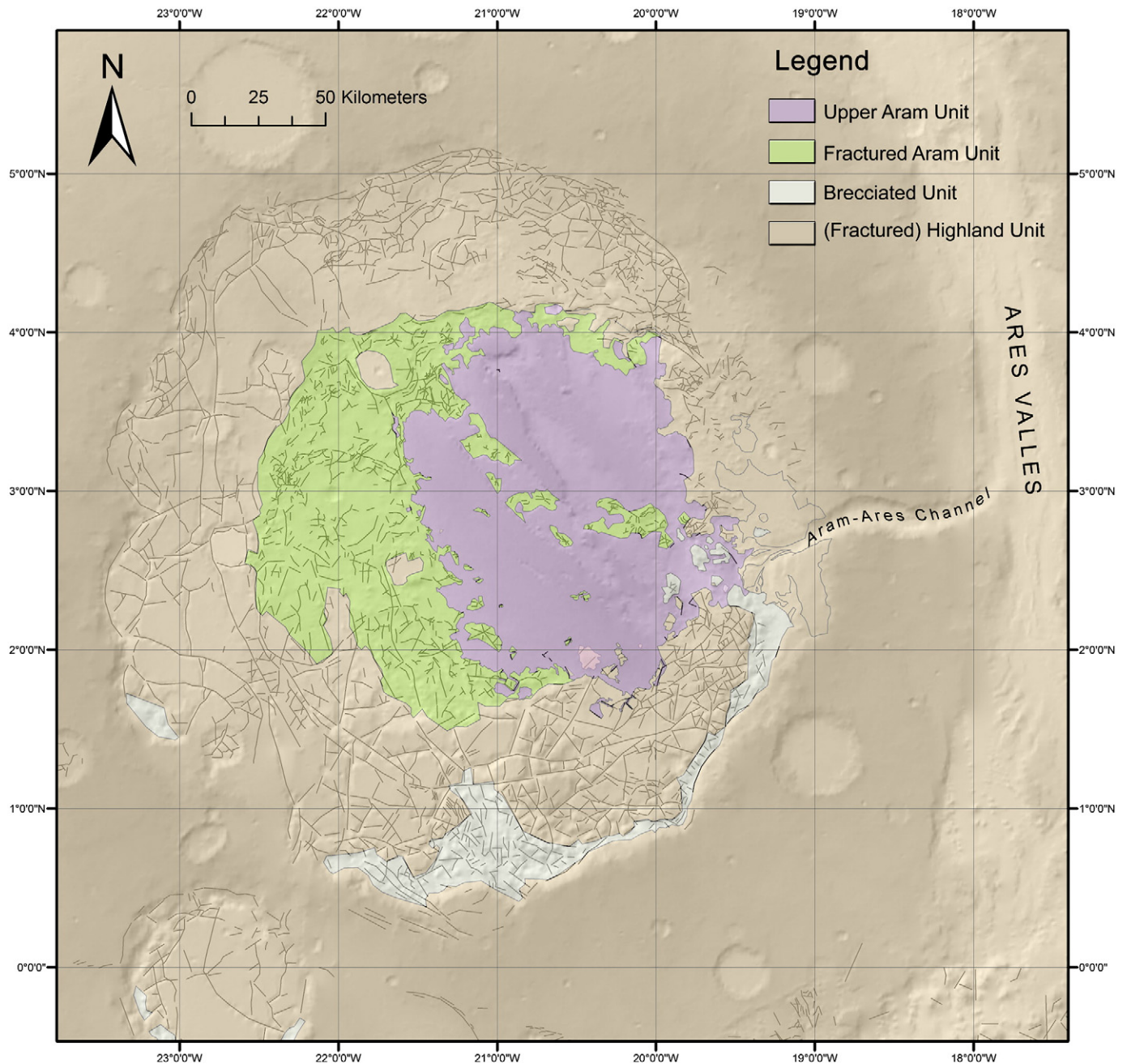


Fig. 2. Simplified geological map of Aram Chaos. The background image is a THEMIS mosaic. The geological map is based on a combination of data from various orbiter instruments: HRSC (Mars Express), in particular 3D visual information derived from stereo images with an image resolution of 12 m/pixel and HRSC Digital Elevation Models, THEMIS (Mars Odyssey), and MOLA (Mars Global Surveyor). All data sets were acquired through the Planetary Science Archive (ESA) and the Planetary Data System (NASA), processed and placed in ArcGIS for mapping and analysis. Note the circular outline of the fractured chaotic terrain and the single outflow channel from Aram Chaos into Ares Vallis. The youngest stratigraphic units in the central part of Aram Chaos are not fractured, i.e. post-date the formation of the chaotic terrain (Glotch and Christensen, 2005) and contain hydrated minerals (Masse et al., 2008).

case, we assume that the entire crater was filled prior to collapse, the amount of subsidence was ~ 2 km. Therefore, the thickness of the liquid water layer was ~ 2 km, and in the scenario we follow, this means that the original ice unit was at least 2 km (not all ice did necessarily melt and moreover the change in volume at the transition from ice to water has to be considered). The thickness of the sedimentary fill of the crater, overlying the ice unit would have varied, growing with time to a maximum of 2 km if the ice unit was 2 km thick (lowest estimate) and the entire crater was filled at some stage prior to collapse.

It is important to consider the potential timing of those processes. We have no direct way to determine the time of

formation of the original impact crater, but for a crater of that size it is likely that the impact took place in the Noachian (>3.7 Ga). The outflow event of the Aram–Ares Channel has not been directly dated, but crater count surface ages from Ares Vallis indicate that outflow events started at 3.6 Ga, and lasted, with several intermittent outflow events, up to the late Hesperian (Warner et al., 2009). Another relative constraint on the timing of the chaos-forming event comes from the light tones layered deposits which unconformably cover the fractured terrain (Masse et al., 2008). However, a firm age constraint for those deposits is lacking. Overall, it is likely that the crater was formed in the Noachian and the chaos-forming event, associated with outflow and channel

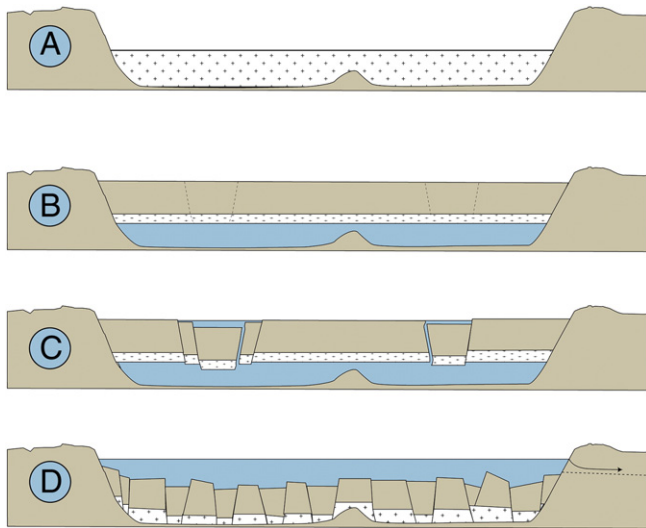


Fig. 3. Conceptual scenario based on the hypothesis that chaotic terrains may form by melting of a subsurface ice unit (Manker and Johnson, 1982), applied to Aram Chaos. Stage A shows the initial condition, with a large impact crater, partly filled with an ice unit. Stage B shows the situation where the ice unit is buried under sediments which filled in the crater depression. If part of the ice unit melts, the situation would eventually become unstable (Stage C), leading to collapse and fracturing of the entire overburden (Stage D). If outflow of water occurs, a channel will be carved (arrow in D). Alternatively, the water may evaporate or freeze. The chaotic terrain will only be visible at the surface if the water evaporates and/or flows out.

formation, took place in the Hesperian. The two events may have been separated by several 100 Myr, up to 1 Gyr.

Erosion and sedimentation rates would have been much higher in the Noachian than in the Hesperian (Hynek and Phillips, 2001), with suggested Noachian sedimentation rates of 1–10 mm/yr. Even at a very low sedimentation rate of 0.01 mm/yr, the 2 km sediment fill could be achieved in 200 Myr. The composition of the basin fill is likely to be a mix of aeolian sediments, impact ejecta, possibly water laid sediments, transported through valley networks, and volcanic airfall sediments. Even lava flows and ice deposits cannot be excluded.

We have no hard constraint on the surface temperature in the Late Noachian and Early Hesperian. Argon thermochronology of Martian meteorites suggests that the surface temperature was below 0 °C since 4 Ga (Shuster and Weiss, 2005). In our modelling we assume that the surface conditions are similar to present day, with an average surface temperature at the equator of -40 °C.

4. Model

The thermal models used for the study are based on a two-dimensional, axis-symmetric cross-section through the crater. A schematic view of the model set-up is shown in Fig. 5. The initial thickness of the ice layer is 2 km in all models, while the thickness of

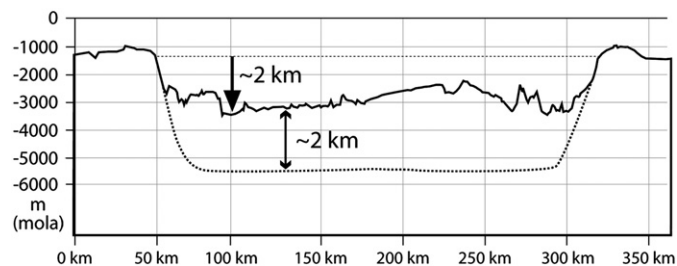


Fig. 4. Topographic cross-section through Aram Chaos (see Fig. 2 for location), based on the gridded MOLA Digital Elevation Model. The outline of the original depth of the Aram Chaos crater is shown with a dashed line, using an empirical crater depth–diameter relation. The original depth of the crater is estimated to have been 4 km.

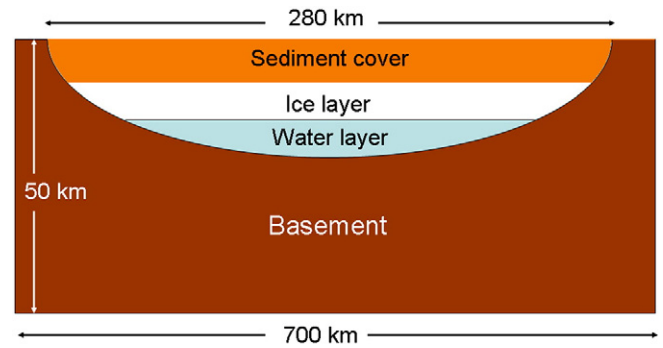


Fig. 5. Schematic model set-up for the thermal numerical modelling of burial of water ice on Mars.

the sediment cover is varied between 0 m and 2000 m. The thickness of the water layer depends only on the amount of melting which occurs and is 0 m at the beginning of the calculations.

For our models we used the commercial software COMSOL Multiphysics®. Only the conductive heat transfer through the different layers was taken into account. No dynamic effects were considered, since the sedimentation rate was less than 1 mm per 1000 years (Smith et al., 2008) we assume that the whole system was always in thermal equilibrium. Thus, only the heat conduction equation was solved for our steady-state models.

The controlling parameters of the models are the thickness of the sediment, its thermal conductivity and the surface heat flux. Radioactive decay within the crust is negligible in comparison to the overall heat flux, and has not been taken into account in our models. Therefore the heat flux is assumed to be constant with depth in the undisturbed host-rock. The temperature distribution in and adjacent to the crater and crater fill is modelled by first determining the temperature at the base of our model (50 km depth) associated with the relevant heat flux. The temperature at the base of the model and the surface temperature (-40 °C in all scenarios) is then kept fixed for each scenario. The temperature distribution is subsequently determined for each stage of crater fill. Thermal insulation has been chosen as boundary condition for the left and right sides, i.e. no heat transport occur across those boundaries. Moreover, the model domain boundary was chosen such that the sides are far enough away from the crater as not to influence the thermal processes there.

In our models the temperature increase within the ice layer due to the pressure of the overlying sediment has been neglected. On Mars, this pressure increase is comparatively small as the gravity is just about 1/3 of the Earth's. Moreover, the phase diagram of water shows that the solidus is much more sensitive to an increase in temperature than in pressure. Therefore, it is valid to neglect the pressure effect on the quantity of ice melt, especially since other parameters (e.g. heat flux, thermal conductivity) have a much larger influence on the melting behaviour of the ice.

One parameter which is important but unfortunately also only poorly constrained is the thermal conductivity of the sediment. The thermal conductivity depends on the composition and on the porosity. Although the crater fill material is probably of basaltic composition, its porosity is undetermined. Due to self-compaction the porosity is likely to decrease with depth, leading to an increase in thermal conductivity. In our model we chose to use a constant thermal conductivity value within the crater fill material. Although this is not realistic, it serves to clearly illustrate the effect of different thermal conductivities within reasonable boundary values. The thermal conductivity at several hundred meters depth is higher than the small values of $0.001 \text{ Wm}^{-1} \text{ K}^{-1}$ to $0.5 \text{ Wm}^{-1} \text{ K}^{-1}$ proposed for Martian surface materials (Mellon et al., 2000). Therefore we used a minimum value of $1 \text{ Wm}^{-1} \text{ K}^{-1}$. The maximum value we used is given by the thermal conductivity of the basement, which is taken to

be $2 \text{ Wm}^{-1} \text{ K}^{-1}$, based on the data by Clifford and Fanale (1985) for solid basaltic rock. The thermal conductivity of the ice was modelled by employing the following equation:

$$k_{\text{ice}}(T) = 567/T,$$

which assumes pure water ice. For the temperatures in our models the effective thermal conductivity is between 2.08 and $2.43 \text{ Wm}^{-1} \text{ K}^{-1}$ (parametrization following Klinger, 1981) and therefore even slightly higher than that of the basement. The melting point of the ice was taken to be 273.15 K in accordance of our assumption of pure water ice. A contamination of the ice by rock or salts might decrease this melting point significantly but as the amount of a potential contamination cannot be determined; this effect was not taken into account.

We used a reference case with a value of $1.4 \text{ Wm}^{-1} \text{ K}^{-1}$ for the thermal conductivity of the sediment and a surface heat flux of 25 mW m^{-2} , and studied the effects of varying the thermal conductivity and heat flux. The different scenarios that we modelled for increasing sediment thicknesses of 0, 500, 1000, 1500 and 2000 m are:

- Scenario 1: heat flux 15 mW m^{-2} , thermal conductivity of overburden $1.4 \text{ Wm}^{-1} \text{ K}^{-1}$
- Scenario 2: heat flux 25 mW m^{-2} , thermal conductivity of overburden $2 \text{ Wm}^{-1} \text{ K}^{-1}$
- Scenario 3 (ref): heat flux 25 mW m^{-2} , thermal conductivity of overburden $1.4 \text{ Wm}^{-1} \text{ K}^{-1}$
- Scenario 4: heat flux 25 mW m^{-2} , thermal conductivity of overburden $1 \text{ Wm}^{-1} \text{ K}^{-1}$
- Scenario 5: heat flux 40 mW m^{-2} , thermal conductivity of overburden $1.4 \text{ Wm}^{-1} \text{ K}^{-1}$

5. Results

For each of the scenarios the thermal modelling resulted in cross-sections through the crater, showing the isotherms with respect to the lithological boundaries governed by the original crater geometry, the ice sheet and the overburden accumulation. An example of such a thermal cross-sections is shown in Fig. 6 for the reference case (Scenario 3) for one side of the crater. In the initial situation, where the crater is partly filled with a 2 km ice sheet, the cryosphere extends to about 3 km depth in both the crater and in the adjacent crust. When the ice sheet is covered by 1500 m of cover material, the isotherms under the crater have warped up due to the insulating effect of the overburden material, with a lower thermal conductivity ($1.4 \text{ Wm}^{-1} \text{ K}^{-1}$) than the surrounding basement ($2 \text{ Wm}^{-1} \text{ K}^{-1}$). As a consequence, the lower part of the ice sheet is no longer situated in the cryosphere, and reaches a temperature above the melting temperature of water. This leads to meta-stable layering in the crater with a basal sheet of liquid water, covered by the remaining ice, covered by sediments. When the entire crater is filled, the liquid water thickness is 1454 m in this particular scenario.

The same principle applies to the other scenarios and the results have been summarized in Fig. 7. The results have been represented in the form of pressure–temperature paths, as is customary in metamorphic studies. The P/T diagram shows the melting curve of pure water (the boundary between the white and the blue field) and for each scenario the resulting curve for a point in the centre of the crater, at the base of the ice sheet. For the reference scenario (scenario 3) point A represents the condition at the surface of the 2 km thick ice sheet before any sediment accumulation. Point A' represents the conditions at the base of the 2 km thick ice sheet in the absence of overburden sediments. As the sediments accumulate (see horizontal lines), the pressure and temperature at the base of the ice sheet increases. At $\sim 750 \text{ m}$ overburden (point B) the base of the ice sheet

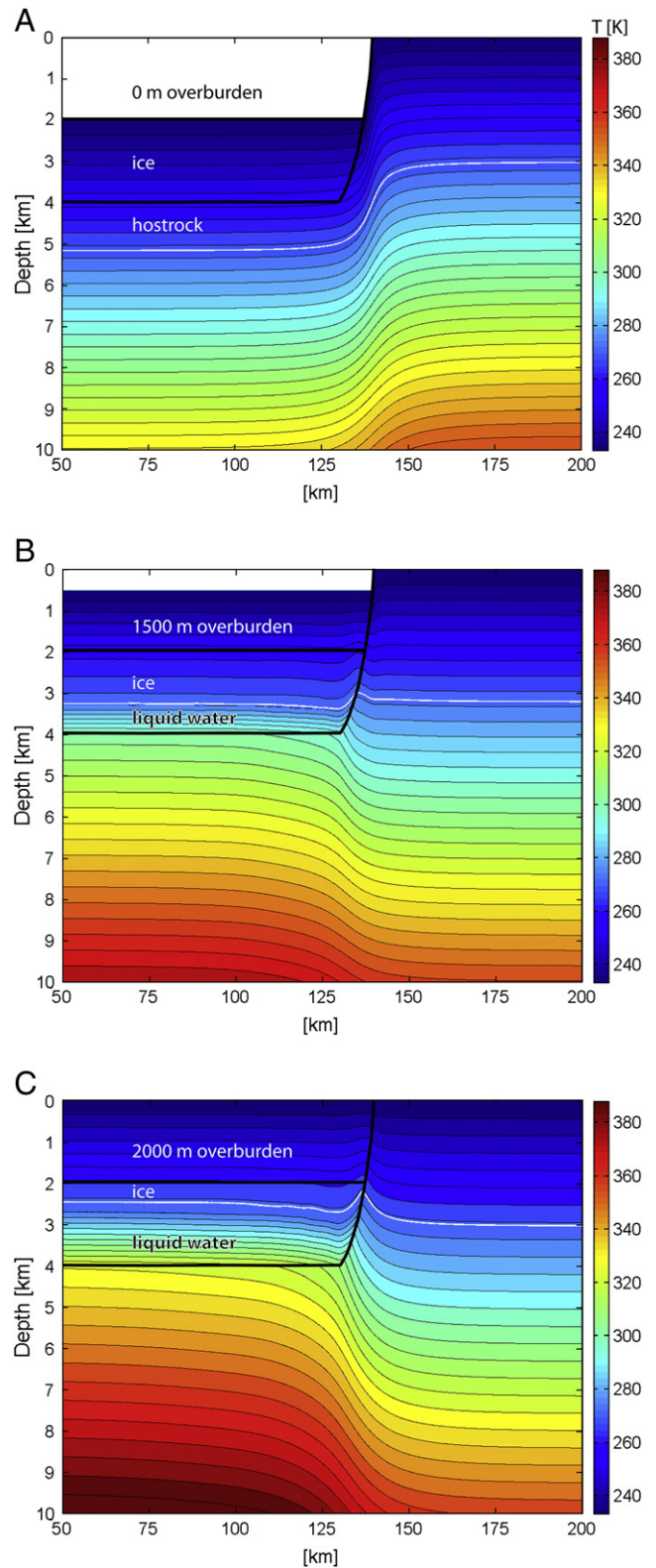


Fig. 6. Temperature distribution in one side of the crater basin for the reference case (scenario 3) with 2000 m of ice, for A) 0 m overburden, B) 1500 m overburden, C) 2000 m overburden. The white line denotes the 273.15 K isotherm, the melting temperature of pure water ice, and the thick black lines give the outlines of the model set-up (crater floor, wall, and sediment/ice interface).

reaches the melting curve. With more sediments accumulating, the amount of melt increases to 116 m for 1000 m overburden, 731 m for 1500 m overburden and finally to 1454 m for a completely filled

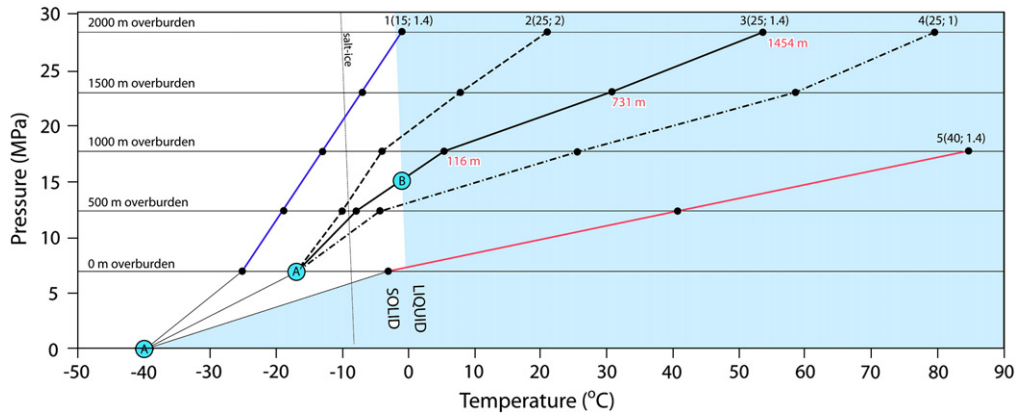


Fig. 7. Modelled pressure–temperature (P/T) paths for a subsurface ice unit under different scenarios, placed in the phase diagram for water. For each scenario in black print: Scenario number (surface heat flux in mW m^{-2} , thermal conductivity of overburden in $\text{Wm}^{-1} \text{K}^{-1}$). Point A represents the starting condition of ice at the surface (-40°C , 700 Pa). The base of the 2 km thick ice unit is modelled for different surface heat flux and thermal conductivity of the overburden. The starting P/T conditions are shown for the base of the ice sheet for 0 m overburden (A'). The P/T conditions for the various scenarios are modelled, always for the base of the ice sheet, in the middle of the crater. In scenario 2, 3, and 4 the melting curve is reached for overburdens between 500 and 1500 m, the stage represented by point B. Scenario 1 just reaches the stage of melting for 2000 m overburden. For scenario 3 the thickness of the layer of melt is shown in red print for overburdens of 1000, 1500, and 2000 m. The dotted line shows the qualitative effect on the melting curve of ice contaminated by salt.

crater. For scenario 5, with a higher heat flux of 40 mW m^{-2} , basal melting starts for an overburden of less than 100 m. In scenario 1, with the lowest heat flux of 15 mW m^{-2} , the melting curve is barely reached for a completely filled crater.

The effect of the thermal conductivity of the overburden is best illustrated by comparing scenario 2, 3 (reference), and 4. A lower thermal conductivity of $1 \text{ Wm}^{-1} \text{K}^{-1}$ (scenario 4) enhances melting of the ice sheet: less overburden is required to start melting, and a thicker melt layer is produced for 2 km overburden. A higher thermal conductivity of the overburden of $2 \text{ Wm}^{-1} \text{K}^{-1}$ (scenario 2) reduces melting: melting starts for a thicker overburden ($>1000 \text{ m}$).

6. Discussion

Can the thermal consequences of burial of ice sheets in pre-existing depressions, such as craters, account for the formation of chaotic terrains and associated catastrophic outflow channels? The key ingredients for the scenario that we hypothesize are plausible for Noachian to Hesperian Mars. The current highland topography attests to a situation where many closed or partially linked depressions occur as a consequence of impact cratering. It is indeed likely that such impact geometries also exist in the subsurface as suggested by Rodriguez et al. (2005a). Build-up of thick equatorial ice sheets in the Noachian, critical to the mechanism we propose, may have been the result of long high obliquity periods (Jakosky and Carr, 1985; Mischna et al., 2003; Head et al., 2005), or alternatively may represent paleopolar ice, deposited prior to true polar wander associated with the rise of the Tharsis bulge (Schultz and Lutz, 1988). In any case, with an average surface temperature below 0°C (Shuster and Weiss, 2005) since 4 Ga, and water ice currently being abundant on the surface of Mars (Head et al., 2003; Plaut et al., 2007; Watters et al., 2007; Holt et al., 2008), ice sheets were also likely in the late Noachian and Hesperian. The deposition of a sedimentary overburden on ice sheets in depressions is the unavoidable counterpart of erosion and denudation (Hynek and Phillips, 2001). Although sedimentation rates were higher in the Noachian, even very low sedimentation rates of $<1 \text{ mm/yr}$ would have been sufficient to fill a deep (2 km) depression given sufficient time (100 Ma to 1 Ga).

The thermal modelling results show that burial of substantial pure water ice sheets is only possible if the surface heat flux is sufficiently low. In the scenarios that we tested, a heat flux of 40 mW m^{-2} led to basal melting starting with less than 100 m overburden. This is equivalent to the situation we have on Earth, where the heat flux is

usually even higher. Under those circumstances, buried water ice would melt before a consolidated overburden formed, resulting in water expulsion and soft sediment deformation (e.g. thaw slumps) in contrast to fracturing and collapse seen in chaotic terrains. Conversely, if the surface heat flux is very low (e.g. scenario 1, 15 mW m^{-2}) within limits of a realistic thickness of overburden the water melting curve is not reached. This means that ice sheets, if they are present in the upper 4 km of the crust, are stable against melting for these conditions.

For an intermediate surface heat flux, between 15 and 40 mW m^{-2} we have the situation where a thick overburden ($>500 \text{ m}$) accumulates before basal melting of the ice sheet occurs, but within realistic overburden thicknesses a substantial part of the ice sheet melts ($>500 \text{ m}$). Under those conditions the scenario that we modelled may lead to the formation of chaotic terrains and outflow channels.

In our modelling we have only considered pure ice. If the ice sheet contains salt, the melting temperature is considerably reduced by about 1.5–1.9 K per mol salt per kg water (Brass, 1980), and the melting curve in Fig. 7 shifts to lower temperatures. The effect is that under similar conditions (surface temperature and heat flux) more melt is produced. Ice contaminated by salt is only likely if the ice sheet originated as a salty lake. If the ice sheet formed by meteoric deposition (snow), the composition of the ice sheet is likely to have been close to pure water, similar to the current polar caps.

The surface heat fluxes we considered are low compared to those (30 mW m^{-2} to 60 mW m^{-2}) suggested by other studies for Mars summarized by Grott and Breuer (2008). However, those studies consider the Noachian period, whereas the values we used could be considered relevant to the Hesperian, at time when the catastrophic outflow channels formed. If our model for the formation of chaotic terrains is correct, the amount of subsidence, i.e. the thickness of the melt layer, can be used as a gauge for the paleo-heat flux. This will require more refined modelling of specific chaotic terrains, including time-dependent aspects such as convection in the buried water lake, and preferably constraints on the thermal conductivity of the overburden. The approach we employed here is conservative in the sense that it shows that even for low heat flux and only thermal diffusion the scenarios may result in substantial melt production.

Fig. 8 shows the phase diagram of water with the schematic P/T path of a particle at the base of the ice sheet during burial and eventually collapse following the modelled reference scenario 3. During burial of the ice sheet the pressure and temperature in the ice sheet increase, until the base of the ice sheet starts to melt (stage B).

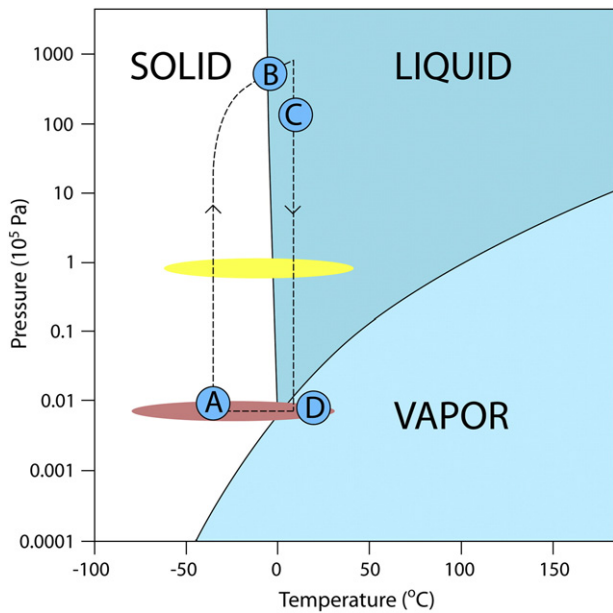


Fig. 8. Phase diagram of water schematically showing the P/T path of an ice particle at the base of the ice sheet during burial and collapse, following the reference Scenario 3. The red field indicates the present surface conditions on Mars, the yellow field the present surface conditions on Earth. Stages A to D refer to the stages of ice burial and collapse shown in Fig. 3.

An important requirement for eventual catastrophic water expulsion to occur is that the subsurface water unit must have stayed in place, first as ice, and subsequently with an increasing basal layer of liquid water. To achieve a thick (>1 km) subsurface lake under slow Martian sedimentation rates of $\sim 10^{-5}$ m/yr, the situation has to remain stable for several 100 millions of years. This is only possible if the liquid water is contained in the subsurface, and does not escape through pore space and cracks in the surrounding solid rocks and ice. To fully evaluate the stability of such a subsurface lake a mechanical modelling study (analogue or numerical) is required. But as an initial indication, we analyzed the lithological and thermal environment in which the growing subsurface lake is situated (Figs. 3 and 6).

The lid of the lake is formed by solid ice until all ice has melted. Under geologic timescales and at temperatures close to the melting temperature, water ice is extremely ductile and behaves like a viscous fluid, analogous to salt units in the subsurface on Earth (Hudec and Jackson, 2007). The ice lid therefore acts as an impermeable layer to the liquid water, closing any permeability that may form by cracks in the overburden. This is particularly important because the transition for ice to liquid water is associated with volume loss. Therefore, basal melting of the ice unit as a consequence of accumulation of overburden will cause a small continuous amount of subsidence in the basin (on the order of 10^{-6} m/yr). Any cracks or fractures associated with such subsidence will be closed in or around the ductile ice unit. In analogy to subsurface salt units on Earth, a subsurface ice unit on Mars has a lower density than the overburden, under certain conditions making the ice unit prone to diapiric rise. Diapiric rise is however only possible if a hydraulic head gradient exists (by a differential overburden), and if space is created by crustal deformation in the overburden (typically by crustal extension) for the low density material to flow upward (Hudec and Jackson, 2007). The slow sedimentation rate in Martian basins is likely to have been homogeneous, avoiding large differential loads. In the absence of plate tectonic stresses, the overburden is not likely to have been breached by diapiric stresses alone.

The liquid water to the sides and bottom of the subsurface lake is in direct contact with rocky material at a temperature above the

melting curve (Fig. 6). The rocky material is likely to consist of a mix of volcanic material, sediments and impact ejecta. Even if a very high (20–30%) initial surface porosity is assumed for such material, at 4 km depth porosity will have been reduced to $\sim 5\%$ due to self-compaction and closure of pore space (Clifford, 1993). Only if porosity is sufficiently high at 4 km depth, if porosity is interconnected to produce sufficient permeability, and if permeability is pervasive all the way to a discharge area, would it be possible for the subsurface lake to drain and discharge through such a subsurface aquifer. Drainage of the subsurface lake in this situation would only occur if the hydraulic head between the subsurface lake and discharge area is such that the flow direction is away from the subsurface lake. In most cases however, the hydraulic head would be such that the subsurface flow direction is into the subsurface lake, since the lake is situated below a topographic depression.

We conclude that for Mars, in contrast to Earth, the slow accumulation of overburden on ice in a confined basin, resulting in a P/T path leg from phase A to B in Fig. 8, may have been metastable for long periods of time (100 Ma–1 Ga).

Breaching of the overburden will lead to a catastrophic chain of events in which highly pressurized liquid water (30 MPa) is released to the surface, where the ambient pressure may be as low as 700 Pa. This would lead to explosive venting and expulsion of water, resulting in hydrofracturing of the overburden, similar to explosive volcanism or catastrophic dissociation of gas-hydrates on the terrestrial ocean floor (Max and Clifford, 2001). In Fig. 8 this part of the P/T path is shown as the leg B–C–D. Eventually, the consequence of expulsion of water to the surface is the collapse of the rocky overburden, up to 2 km thick. Simultaneously, the newly formed basin would fill with liquid water expelled from the subsurface (Figs. 3 and 8, Phase D). The simplest case that we consider is that all liquid water is drained from the subsurface in one single event. In reality, the mechanics of the system may result in several large outflow events. In addition, the possibility exists that after the first collapse event, a remaining sheet of ice remains in the subsurface, which, after thermal equilibration, melts and results in a renewed catastrophic outflow event. To test such hypotheses, mechanical numerical and analogue models are required.

The hypothesis we propose has elements in common with previously proposed models for the formation of chaotic terrain and catastrophic outflow channels, but it differs in a number of critical aspects. The model studied by Manker and Johnson (1982) in analogue simulations is perhaps the closest to our hypothesis, with chaotic terrains and outflow channels forming by melting of a subsurface ice sheet. However, in all previously proposed models for melting of the cryosphere or subsurface ice sheets, the trigger for melting was thought to be a thermal anomaly induced by volcanism or the intrusion of magma in the subsurface (Meresse et al., 2008). In our thermal modelling we show that melting of a subsurface ice sheet is a self-consistent mechanism, which, by slow and gradual processes such as sedimentation and thermal adjustment around buried ice, may lead to the catastrophic events associated with expulsion of large quantities of water from the subsurface.

Our hypothesis differs from the set of models which advocate the formation of outflow channels by discharge from a pressurized sub-cryosphere aquifer (Carr, 1979; Andrews-Hanna and Phillips, 2007; Harrison and Grimm, 2008, 2009). Aquifer models suppose and require the existence of a thick (up to 20 km) highly permeable layer in the Martian crust from which water is discharged into a topographic low. A pre-existing topographic low is required to produce the hydraulic head needed to breach the cryosphere and produce discharge in those models. It is challenging to explain the large scale fracturing and subsidence

over 1–2 km in chaotic terrains by water discharge from an aquifer. Subsidence is a direct consequence of the removal of subsurface material, most likely water in this case. Discharge from pore space relies on flow of water through a permeable subsurface layer, where water that is discharged is replaced by recharge. For Martian aquifer models recharge is generally assumed from ice caps at great distance (>2000 km) (Clifford, 1993; Harrison and Grimm, 2008). Since little net material is removed from the subsurface in such a scenario, subsidence is not a likely consequence of an aquifer. In fact, fracturing, collapse and subsidence of an aquifer would severely reduce the permeability of the aquifer, preventing or reducing further discharge. Although the model that we propose for chaotic terrain formation does not require a sub-cryosphere aquifer to be present, the presence of an aquifer is no impediment to the mechanism we propose.

On theoretical grounds our study shows that the mechanism of burial and melt of ice sheets on Mars is plausible, but the test of this hypothesis is in the match between the predicted geological features and events, and the observations recorded in Martian chaotic terrains and outflow channels. Each chaotic terrain on Mars has unique geological and morphological features. Here we limit ourselves to the first order model predictions and observations shared by most chaotic terrains.

From our hypothesis we predict simultaneous subsidence, fracturing and expulsion of water from the subsurface in a catastrophic manner. This is at first order consistent with geological features and sequences of events reported for chaotic terrains (Rodriguez et al., 2006; Meresse et al., 2008). The volume of liquid water released from the subsurface in a very short time is predicted to $\sim 10^4$ km³ for Aram Chaos (a 2 km layer of liquid water in a 280 km diameter crater). This is consistent with volumes of $\sim 10^5$ – 10^6 km³ required to carve the large outflow channels such as Ares Valles, which are sourced by larger and multiple chaotic terrains (Baker, 2001). To further test this hypothesis multiple chaotic terrains and their associated outflow channels should be studied and modelled. At the moment, subsurface imaging techniques are insufficiently developed for Mars to allow the detection of liquid water or ice below a thick (>100 m) rocky sequence. The penetration of radar waves from the MARSIS and SHARAD instruments is sufficient to image subsurface features in ice, but not through rock (Cereti et al., 2007). In the future, new instrumental techniques such as seismic interferometry, may allow for testing of this hypothesis by subsurface imaging techniques. The subsurface of Mars may in theory still contain buried ice sheets, potentially even with a basal melt layer.

7. Conclusions

On the grounds of theoretical considerations and 2D thermal modelling we conclude that burial of ice sheets in a confined basin on Mars, resulting in basal melting with sufficient thickness of overburden, is a plausible mechanism for the formation of chaotic terrains. In this hypothesis, the chaotic terrain, and an associated outflow channel form when such a subsurface lake collapses and highly pressurized liquid water is expelled to the surface in a catastrophic manner. Basal melting in this hypothesis is a direct consequence of the insulating effect of the overburden. There is no need to invoke a thermal event in the crust to trigger melting.

This mechanism is plausible if the surface temperature is low (-40 °C in our model) and the crustal heat flux is low (between 15 and 40 mW m⁻²). On Earth such conditions never existed, hence this hypothesis implicitly provides an explanation for the lack of chaotic terrains on Earth, whereas on Mars they form an important terrain type.

Acknowledgements

We thank Keith Harrison, Victor Baker, Hans de Bresser, Rachel Walcott, Ernst Hauber and Cor Langereis for reviews of early versions of the manuscript, and we thank Matthias Grott and Timothy Glotch for constructive reviews of this paper.

References

- Andrews-Hanna, J.C., Phillips, R.J., 2007. Hydrological modeling of outflow channels and chaos regions on Mars. *J. Geophys. Res.* 112. doi:10.1029/2006je002881.
- Baker, V.R., 2001. Water and the martian landscape. *Nature* 412, 228–236.
- Brass, G.W., 1980. Stability of brines on Mars. *Icarus* 42, 20–28.
- Carr, M.H., 1979. Formation of Martian flood features by release of water from confined aquifers. *J. Geophys. Res.* 84, 2995–3007.
- Carr, M.H., 1980. The morphology of the Martian surface. *Space Sci. Rev.* 25, 231–284.
- Carr, M.H., 1996. *Water on Mars*. Oxford Univ. Press, New York.
- Catling, D.C., Moore, J.A., 2003. The nature of coarse-grained crystalline hematite and its implications for the early environment of Mars. *Icarus* 165, 277–300.
- Cereti, A., et al., 2007. Electromagnetic measurements on Martian soil analogs: implications for MARSIS and SHARAD radars in detecting subsoil water. *Planet. Space Sci.* 55, 193–202.
- Chapman, M.G., Tanaka, K.L., 2002. Related magma–ice interactions: possible origins of chasmata, chaos, and surface materials in Xanthe, Margaritifer, and Meridiani Terrae, Mars. *Icarus* 155, 324–339.
- Christensen, P.R., Morris, R.V., Lane, M.D., Bandfield, J.L., Malin, M.C., 2001. Global mapping of Martian hematite mineral deposits: remnants of water-driven processes on early Mars. *J. Geophys. Res.* 106, 23873–23885.
- Clifford, S.M., 1993. A model for the hydrologic and climatic behavior of water on Mars. *J. Geophys. Res.* 98, 10973–11016.
- Clifford, S., Fanale, F., 1985. The thermal conductivity of the Martian crust. 16th Annual Lunar and Planetary Science Conference, pp. 144–145. Houston.
- Gendrin, A., et al., 2005. Sulfates in Martian layered terrains: the OMEGA/Mars Express view. *Science* 307, 1587–1591.
- Glotch, T.D., Christensen, P.R., 2005. Geologic and mineralogical mapping of Aram Chaos: evidence for a water-rich history. *J. Geophys. Res.* 110.
- Glotch, T.D., Rogers, A.D., 2007. Evidence for aqueous deposition of hematite and sulfate-rich light-toned layered deposits in Aureum and Iani Chaos, Mars. *J. Geophys. Res.* 112, E06001. doi:10.1029/2006je002863.
- Grott, M., Breuer, D., 2008. Constraints on the radiogenic heat production rate in the Martian interior from viscous relaxation of crustal thickness variations. *Geophys. Res. Lett.* 35. doi:10.1029/2007g033021.
- Harrison, K.P., Grimm, R.E., 2008. Multiple flooding events in Martian outflow channels. *J. Geophys. Res.* 113. doi:10.1029/2007je002951.
- Harrison, K.P., Grimm, R.E., 2009. Regionally compartmented groundwater flow on Mars. *J. Geophys. Res.* 114. doi:10.1029/2008je003300.
- Head, J.W., et al., 2003. Recent ice ages on Mars. *Nature* 426, 797–802.
- Head, J.W., et al., 2005. Tropical to mid-latitude snow and ice accumulation, flow and glaciation on Mars. *Nature* 434, 346–351.
- Holt, J.W., et al., 2008. Radar sounding evidence for buried glaciers in the southern mid-latitudes of Mars. *Science* 322, 1235–1238.
- Hudec, M.R., Jackson, M.P.A., 2007. Terra infirma: understanding salt tectonics. *Earth Sci. Rev.* 82, 1–28.
- Hynek, B.M., Phillips, R.J., 2001. Evidence for extensive denudation of the Martian highlands. *Geology* 29, 407–410.
- Jakosky, B.M., Carr, M.H., 1985. Possible precipitation of ice at low latitudes of Mars during periods of high obliquity. *Nature* 315, 559–561.
- Klinger, J., 1981. Some consequences of a phase transition of water ice on the heat balance of comet Nucei. *Icarus* 47, 320 pp.
- Lichtenberg, K.A., Arvidson, R.E., Morris, R.V., Murchie, S.L., Bishop, J.L., Glotch, T.D., Dobre, E.N., Mustard, J.F., Andrews-Hanna, J., Roach, L.H., the CRISM team. 2010. Stratigraphy of hydrated sulfates in the sedimentary deposits of Aram Chaos, Mars. *J. Geophys. Res.* 115, E00D17. doi:10.1029/2009je003353.
- Manker, J.P., Johnson, A.P., 1982. Simulation of Martian chaotic terrain and outflow channels. *Icarus* 51, 121–132.
- Masse, M., et al., 2008. Mineralogical composition, structure, morphology, and geological history of Aram Chaos crater fill on Mars derived from OMEGA Mars Express data. *J. Geophys. Res.* 113. doi:10.1029/2008je003131.
- Max, M.D., Clifford, S.M., 2001. Initiation of Martian outflow channels: related to the dissociation of gas hydrate? *Geophys. Res. Lett.* 28, 1787–1790.
- Mellon, M.T., et al., 2000. High-resolution thermal inertia mapping from the Mars Global Surveyor Thermal Emission Spectrometer. *Icarus* 148, 437–455.
- Meresse, S., et al., 2008. Formation and evolution of the chaotic terrains by subsidence and magmatism: Hydrates Chaos, Mars. *Icarus* 194, 487–500.
- Mischna, M.A., et al., 2003. On the orbital forcing of Martian water and CO₂ cycles: a general circulation model study with simplified volatile schemes. *J. Geophys. Res.* 108. doi:10.1029/2003je002051.
- Montgomery, D.R., Gillespie, A., 2005. Formation of Martian outflow channels by catastrophic dewatering of evaporite deposits. *Geology* 33, 625–628.
- Nelson, D., Greeley, R., 1999. Geology of Xanthe Terra outflow channels and the Mars Pathfinder landing site. *J. Geophys. Res.* 104, 8653–8670.

- Noe Dobrea, E.Z., Poulet, F., Malin, M.C., 2008. Correlations between hematite and sulfates in the chaotic terrains east of Valles Marineris. *Icarus* 193, 516–534.
- Parker, M.V.K., Zegers, T., Kneissl, T., Ivanov, B., Foing, B., Neukum, G., 2010. 3D structure of the Gusev Crater region: Earth and Planetary Science Letters 294(3–4), 411–423. doi:10.1016/j.epsl.2010.01.013.
- Plaut, J.J., et al., 2007. Subsurface radar sounding of the south polar layered deposits of Mars. *Science* 316, 92–95.
- Rodriguez, J.A.P., et al., 2005a. Control of impact crater fracture systems on subsurface hydrology, ground subsidence, and collapse, Mars. *J. Geophys. Res.* 110. doi:10.1029/2004je002365.
- Rodriguez, J.A.P., et al., 2005b. Outflow channel sources, reactivation, and chaos formation, Xanthe Terra, Mars. *Icarus* 175, 36–57.
- Rodriguez, J.A.P., et al., 2006. Headward growth of chasmata by volatile outbursts, collapse, and drainage: evidence from Ganges chaos, Mars. *Geophys. Res. Lett.* 33. doi:10.1029/2005gl024320.
- Schultz, P.H., Lutz, A.B., 1988. Polar wandering of Mars. *Icarus* 73, 91–141.
- Sharp, R.P., 1973. Mars: fretted and chaotic terrains. *J. Geophys. Res.* 78, 4073–4083.
- Shuster, D.L., Weiss, B.P., 2005. Martian surface paleotemperatures from thermochronology of meteorites. *Science* 309, 594–597.
- Smith, M.R., Gillespie, A.R., Montgomery, D.R., 2008. Effect of obliteration on crater-count chronologies for Martian surfaces. *Geophys. Res. Lett.* 35. doi:10.1029/2008GL033538.
- Tanaka, K.L., et al., 2003. Resurfacing history of the northern plains of Mars based on geologic mapping of Mars Global Surveyor data. *J. Geophys. Res.* 108. doi:10.1029/2002JE001908.
- Warner, N., et al., 2009. A refined chronology of catastrophic outflow events in Ares Vallis, Mars. *Earth Planet. Sci. Lett.* 288, 58–69.
- Watters, T.R., et al., 2007. Radar sounding of the Medusae Fossae Formation Mars: equatorial ice or dry, low-density deposits? *Science* 318, 1125–1128.